

Non-ballistic spin separator based on Y-shaped nanostructure with a quantum point contact

P. Wójcik,* M. Wołoszyn, B. J. Spisak, and J. Adamowski
 AGH University of Science and Technology, Faculty of Physics and
 Applied Computer Science, al. Mickiewicza 30, Kraków, Poland

A proposal of a spin separator based on the spin Zeeman effect in Y-shaped nanostructure with a quantum point contact is presented. Our calculations show that the appropriate tuning of the quantum point contact potential and the external magnetic field leads to the spin separation of the current: electrons with opposite spins flow through the different output branches. We demonstrate that this effect is robust against the scattering on impurities. The proposed device can also operate as a spin detector, in which – depending on the electron spin – the current flows through one of the output branches.

PACS numbers: 72.25.Dc

A design of a controllable source of spin-polarized electrons and an efficient injection of the spin-polarized current into a semiconductor is a basic requirement for a fabrication of novel spintronic devices. The original idea of the spin transistor¹ was assumed that spin-polarized charges are injected into semiconductor channel from the ferromagnetic contact. However, due to the conductivity mismatch between the ferromagnetic and semiconductor materials, the efficiency of the spin injection at ferromagnet/semiconductor interface is rather low – experimentally reported at the level of a few percent.^{2–4} The low spin-injection rate results in the low signal in the experimental realization of the spin transistor.⁵ In order to overcome the conductivity mismatch, the spin-polarized current is injected into the semiconductor using the magnetic semiconductors.^{6,7} In the experiments with the magnetic-semiconductor/semiconductor interface, the spin polarization rate reaches the value as high as 90%.^{8–10} Moreover, the use of magnetic semiconductors in resonant tunneling structures allows to construct the spin filter, in which the polarization of the current can be changed from fully spin-down to fully spin-up polarized by the bias voltage.^{11,12} In our recent paper,¹³ we have studied the spin filter effect in the resonant tunneling diode based on ferromagnetic GaMnN and shown that the spin filter operation can be realized even at room temperature. Several alternative methods to achieve the spin-polarizing effect in semiconductor nanostructures have been recently demonstrated in nanowires with spin-orbit interaction,^{14,15} quantum dots,¹⁶ and carbon nanotubes.¹⁷ Although all these devices allow to obtain the spin polarized current, they do not separate the current into the beams with opposite spin. This operation is more complicated and requires the application of the device with at least three terminals: one terminal acts as the input through which the unpolarized current is injected, and the other two terminals act as outputs, through which the spin polarized beams flow out of the device. The spin separation effect in the presence of the spin-orbit interaction has been theoretically predicted in the ballistic T-shaped¹⁸ and Y-shaped^{19,20} structures as well as quantum rings.²¹ The spin-orbit interaction in-

duced by the quantum point contact (QPC) has been recently applied to reproduce the Stern-Gerlach experiment in the two dimensional electron gas (2DEG).^{22,23} However, the operation of the devices based on the spin-

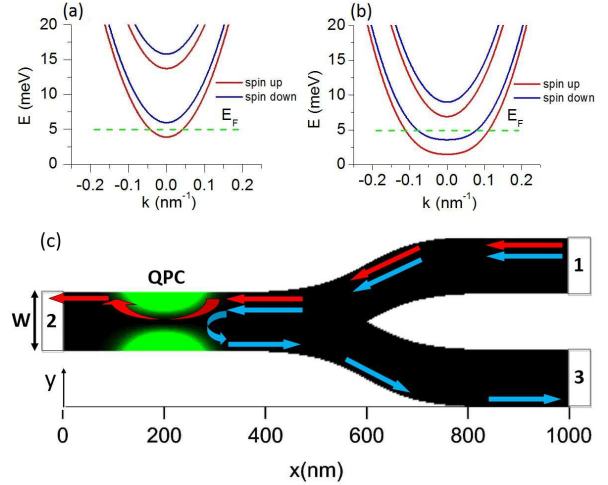


FIG. 1. (a,b) Dispersion relations $E(k)$ for spin-up (red curves) and spin-down (blue curves) electrons calculated for (a) the center of the QPC and (b) the leads. The green horizontal dashed line denotes Fermi energy E_F . (c) Schematic of the Y-shaped nanostructure with the QPC (the green regions illustrate the QPC potential energy profile [cf. Eq. (2)]). The unpolarized current injected from electrode 1 is separated into the two spin-polarized electron beams. Red (blue) arrows depict the currents of the spin-up (spin-down) electrons.

orbit interaction is very sensitive to the scattering processes and can be affected by the spin relaxation according to the Dyakonov-Perel mechanism.²⁴ Therefore, the operation of the spin separator exploiting the spin-orbit interaction is restricted to the ballistic regime, which is a serious obstacle from the experimental point of view. In this letter, we propose the spin separator based on the Y-shaped 2DEG with the QPC located in one of the branches. We show that the proposed nanodevice can be

used both for the separation and detection of the electron spin. Moreover, if the nanodevice operates in the regime, in which the current is carried through the edge states, then – in analogy to the quantum Hall effect – the spin separation is robust against the scattering.

We consider the Y-shaped two-dimensional nanostructure with the QPC located near the contact 2 [Fig. 1(c)]. Experimentally, similar construction but in the quantum ring geometry has been fabricated by the use of the lithography technique.²⁵ In the presence of the external magnetic field $\mathbf{B} = (0, 0, B)$, the Hamiltonian of the system takes on the form

$$\hat{H} = \left[\frac{(-i\hbar\nabla + e\mathbf{A})^2}{2m_e} + U(\mathbf{r}) \right] \mathbf{1} + \frac{1}{2}g\mu_B B\sigma_z, \quad (1)$$

where $\mathbf{A} = (yB, 0, 0)$ is the vector potential, m_e is the conduction-band mass, $\mathbf{1}$ is the 2×2 unit matrix, and σ_z is the z -spin Pauli matrix. Potential energy $U(\mathbf{r}) = U_c(x, y) + U_{QPC}(x, y)$ is the sum of the Y-shaped confinement potential energy $U_c(x, y)$ (we assume the hard-wall confinement in the y direction) and the electron potential energy in the QPC

$$U_{QPC}(x, y) = \frac{1}{2}m_e^2\omega^2 y^2 \exp\left[\frac{-(x-x_0)^2}{2d^2}\right], \quad (2)$$

where d determines the x -extension of the QPC, x_0 defines its position, and $\hbar\omega$ is the energy of the transverse parabolic confinement in the QPC region. We assume that the confinement in the z direction is so strong that electrons occupy the ground-state resulting from the size quantization along this axis. In the calculations, we adopt the following geometrical parameters: width of the channel $W = 40$ nm, length of the nanostructure $L = 1000$ nm, $d = 40$ nm, and $x_0 = 200$ nm. We use the material parameters corresponding to $\text{In}_{0.5}\text{Ga}_{0.5}\text{As}$, i.e. $m_e = 0.0465m_0$ and $g = -8.97$, however the spin separation effect will be observed for any semiconductor material with sufficiently large spin Zeeman splitting. The numerical calculations have been performed using the tight-binding method on the square lattice with $\Delta x = \Delta y = 2$ nm and the hopping energy $t = \hbar^2/(2m_e\Delta x^2)$. We have used the Kwant package²⁶ to determine the spin-dependent conductance $G_{ij}^{u(d)}$ between the contacts i and j ($i, j = 1, 2, 3$, u and d correspond to spin-up and spin-down, respectively). In the proposed nanostructure electrons are injected from the lead 1 acting as the input and flow out from the device via the leads 2 and 3 (see Fig. 1). Figure 2 (upper panels) presents the spin-dependent conductance $G_{ij}^{u(d)}$ as a function of the QPC confinement energy $\hbar\omega$ for magnetic field (a) $B = 1$ T and (b) $B = 3$ T. We see that the rapid decrease of the conductance between the contacts 1 and 2 for the spin-up electrons occurs for the higher energy than for the spin-down electrons. Simultaneously, for both the spin polarizations the decrease of the electron transmission into the channel 2 is accompanied by the increase of the transmission into the channel 3. This means that

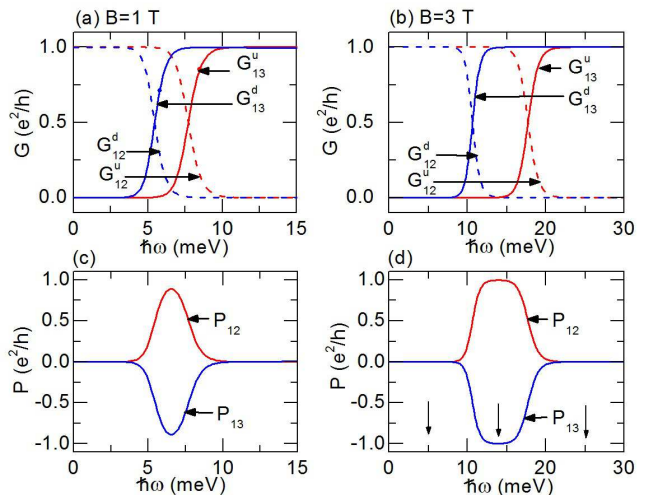


FIG. 2. Spin-up (red curves) and spin-down (blue curves) conductance $G_{ij}^{u(d)}$ as a function of confinement energy $\hbar\omega$ for magnetic field (a) $B = 1$ T and (b) $B = 3$ T. Panels (c) and (d) show the differences of the conductances $P_{12} = G_{12}^u - G_{12}^d$ and $P_{13} = G_{13}^u - G_{13}^d$. In panel (d), the vertical arrows mark the values of $\hbar\omega$ chosen to present the results in Fig. 3.

in the confinement energy regime, for which the conductance of the spin-up electrons through the channel 2 is still high, the spin-down electrons are reflected from the QPC and flow through the channel 3. The current splits into the two spin-polarized beams. The splitting effect is quantitatively presented in Figs. 2 (c,d) which show the differences of the conductances $P_{12} = G_{12}^u - G_{12}^d$ and $P_{13} = G_{13}^u - G_{13}^d$. In Figs. 2 (c,d) the spin separation of the current is revealed as the peak (dip), which corresponds to the spin-up (spin-down) polarization of the current flowing through the corresponding channel.

The spin separation mechanism proposed in this paper results from the joint effect of the spin Zeeman splitting and the formation of edge states. If the magnetic field is applied, the spin degeneration of transverse electron states is lifted by the Zeeman effect [cf. the dispersion relations in Fig. 1 (a,b)]. In the calculations we have adjusted the Fermi level in the leads so that only the two lowest transverse states (one corresponding to spin-up and one corresponding to spin-down) are occupied [see Fig. 1(b)]. The spin-up and spin-down electrons with the chosen energy are injected into the system from the lead 1 and flow towards the QPC located in the channel 2. Due to the spin Zeeman splitting the reflection probabilities in the QPC region for spin-up and spin-down electrons are different. The increase of the confinement energy $\hbar\omega$ leads to the increase of the transverse state energies in the QPC. In particular, we can tune $\hbar\omega$ so that only the spin-up energy level is located below the Fermi energy. [see Fig. 1(a)]. The absence of the available spin-down electron states in the QPC region results in a backscattering of spin-down electrons. On the other hand, the

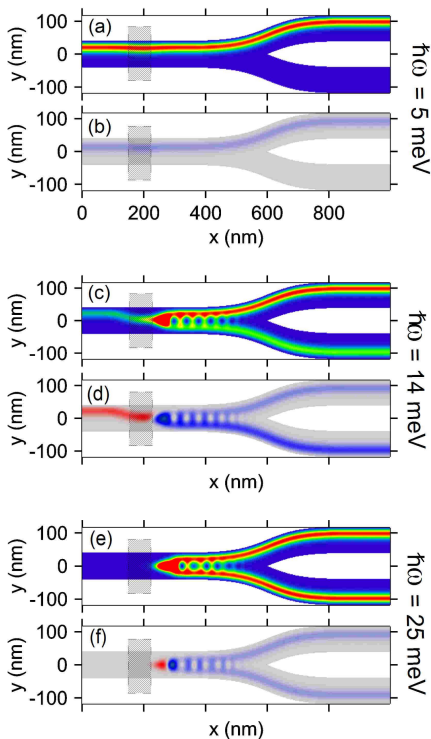


FIG. 3. Electron density (a,c,e) and spin density (b,d,f) in the nanostructure for (a,b) $\hbar\omega = 2$ meV, (c,d) $\hbar\omega = 14$ meV, and (e,f) $\hbar\omega = 25$ meV. The gray rectangle represents the position of the QPC.

spin-up electrons still have a high transmission probability through the QPC. Therefore, the current splits into the two spin-polarized electron beams. In order to obtain the full separation of the electrons with opposite spins we exploit the orbital effect, which causes that the transport of electrons is carried by the edge states that are formed in a sufficiently high magnetic field. Due to the orbital effect, the electrons with negative and positive velocities (along the x -axis) are spatially separated. The electrons flowing in a certain direction are always shifted, by the Lorentz force, to the right boundary of the conductive channel with respect to the direction of the current flow (cf. Fig. 3). This causes that the spin-down electrons backscattered from the QPC are injected into the channel 3. In other words, the orbital effect prevents the spin-down polarized electrons reflected from the QPC to flow back into the channel 1. The resulting spin separation effect is clearly demonstrated in Fig. 3. For $\hbar\omega = 5$ meV both the spin-up and spin-down electrons are transmitted through the QPC [Fig. 3(a)] and reach the contact 2. We see that the current is partially spin polarized [Fig. 3(a)], which is a consequence of unequal electron densities of states at the Fermi level which results from the spin Zeeman effect. For $\hbar\omega = 14$ meV [Fig. 3(b)] the Y-shaped nanostructure acts as the (almost) perfect spin splitter. Depending on their spins the electrons injected

from the contact 1 are either transmitted through the QPC into the channel 2 or reflected into the channel 3. As described above, the backscattering of the spin-down electrons is very strong [cf. Fig. 3(d)]. We have found that the nanodevice with the parameters of Fig. 3(d) is the optimal realization of the spin separator, in which the electrons with the opposite spins are spatially separated and leave the nanostructure via the different conduction channels. The further increase of the confinement energy $\hbar\omega$ [Fig. 3(e,f)] causes that in the QPC region there are no available quantum states for both the spin-up and spin-down electrons. The electrons with either spin are fully reflected from the QPC and due to the orbital effect flow through the channel 3.

The results presented so far have been obtained with the neglect of the scattering. Nevertheless, from the experimental point of view it is desirable to construct the spin selector which acts in the non-ballistic regime. Now, we will show that the nanodevice proposed in our paper is robust against the scattering. Due to the orbital effect, the electrons flowing in a certain channel are moved towards the edge according to the Lorentz force direction. For the sufficiently strong magnetic field, the currents flowing in the opposite directions are transported through the edge states localized at two opposite sides of the channel. If we increase the magnetic field, the separation between edge states carrying the current in the opposite directions increases. This effect leads to the suppression of the backscattering since the electron can change its momentum only if it is scattered from the edge state localized on one side of the channel to that on the other side. The scattering is suppressed due to the vanishingly small overlap between the wave functions localized on the opposite sides of the channel. This mechanism is well known and is the origin of the 'zero' resistance in the quantum Hall effect.²⁷ We have quantitatively described this effect introducing the model according to which the spin-independent scattering is included by assuming that the transfer energy t is uniformly distributed within the range $W/2 < t < W/2$.²⁸ The relation between the strength of scatterers and the mean free path ℓ is given by²⁸

$$\frac{W}{E_F} = \left(\frac{6\lambda_F^3}{\pi^3 \Delta x^2 \ell} \right)^{1/2}, \quad (3)$$

where λ_F is the Fermi wavelength. In our calculations, we have applied the realistic values of the mean free path, which was experimentally measured to be greater than $1\mu\text{m}$ for the 2DEG in InGaAs.²⁹ Fig. 4 shows P_{12} and P_{13} calculated in the non-ballistic regime as a function of $\hbar\omega$ for several values of the mean free path. The results presented in Fig. 4 have been obtained by averaging over 10^4 computational runs for each value of the energy $\hbar\omega$. We see that – in the considered non-ballistic regime – the scattering does not affect the spin-splitting effect. The pronounced peak and dip, which demonstrate spin separation are still clearly visible. We should emphasize that the insensitivity of the scattering becomes greater, if

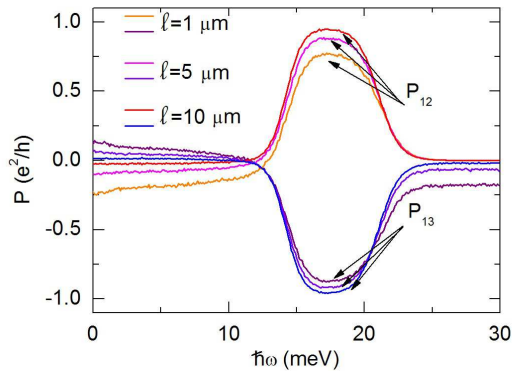


FIG. 4. Spin polarization P_{12} and P_{13} as a function of the QPC confinement energy $\hbar\omega$. Results calculated in the non-ballistic regime for different values of mean free path ℓ .

the external magnetic field increases. Since in this regime the effect of the external magnetic field is dominating, we neglect the spin-orbit interaction in our calculations.

In conclusion, we have proposed the non-ballistic spin separator based on the Y-shaped 2DEG with the QPC. We have shown that by the appropriate tuning of

confinement energy in the QPC, the input unpolarized current can be splitted into two fully spin-polarized beams, whereas the electrons with opposite spins flow through the different branches of the nanostructure. The separation mechanism has been explained as the joint effect of the spin Zeeman splitting and transport via the edge states generated in the external magnetic field. We show that the proposed spin separation mechanism is robust against the scattering. Although the results have been presented as a function of the QPC confinement energy $\hbar\omega$, in the experimental realization this energy can be tuned by changing the voltage applied to the QPC contacts. In this structure the spin separation effect can be easily switched on/off by the change of the voltage applied to the nearby gate. It is also worth noting that if the fully spin polarized current is injected from the input electrode, the current will flow through only one of the output branches. In this case, when measuring the current in both the output, we obtain the information about the spin polarization of the current injected into the system. This means that the proposed nanodevice can also acts as a detector of the spin polarized current.

This work has been supported by the National Science Centre, Poland, under grant DEC-2011/03/B/ST3/00240.

* Electronic address: pawelwojcik@fis.agh.edu.pl

¹ S. Datta and B. Das, *Appl. Phys. Lett.* **56**, 665 (1990).

² P. R. Hammar, B. R. Bennett, M. J. Yang, and J. M. *Phys. Rev. Lett.* **83**, 203 (1999).

³ G. Schmidt, D. Ferrand, L. W. Molenkamp, A. T. Filip, and B. J. van Wees, *Phys. Rev. B* **62**, 4790(R) (2000).

⁴ S. A. Crooker, M. Furis, X. Lou, D. L. Smith, C. J. Palmstrom, and P. A. Crowell, *Science* **309**, 2191 (2005).

⁵ H. C. Koo, J. H. Kwon, J. Eom, J. Chang, S. H. Han, and M. Johnson, *Science* **325**, 1515 (2009).

⁶ T. Dietl, H. Ohno, F. Matsukura, J. Cibert, and D. Ferrand, *Science* **287**, 1019 (2000).

⁷ T. Jungwirth, J. Sinova, J. Mašek, J. Kučera, and A. H. MacDonald, *Rev. Mod. Phys.* **78**, 809 (2006).

⁸ R. Fiederling, M. Keim, G. Reuser, W. Ossau, G. Schmidt, A. Waag, and L. W. Molenkamp, *Nature* **402**, 787 (1999).

⁹ Y. Ohno, D. K. Young, B. Beschoten, F. Matsukura, H. Ohno, and D. D. Awschalom, *Nature* **402**, 790 (1999).

¹⁰ B. T. Jonker, Y. D. Park, B. R. Bennett, H. D. Cheong, G. Kioseoglou, and A. Petrou, *Phys. Rev. B* **62**, 8180 (2000).

¹¹ A. Slobodsky, C. Gould, T. Slobodskyy, C. R. Becker, G. Schmidt, and L. W. Molenkamp, *Phys. Rev. Lett.* **90**, 246601 (2003).

¹² P. Wójcik, J. Adamowski, M. Wołoszyn, and B. J. Spisak, *Phys. Rev. B* **86**, 165318 (2012).

¹³ P. Wójcik, J. Adamowski, M. Wołoszyn, and B. J. Spisak, *Appl. Phys. Lett.* **102**, 242411 (2013).

¹⁴ M. P. Nowak and B. Szafran, *Appl. Phys. Lett.* **103**,

202404 (2013).

¹⁵ P. Szumniak, S. Bednarek, B. Partoens, and F. M. Peeters, *Phys. Rev. Lett.* **109**, 107201 (2012).

¹⁶ J. A. Folk, R. M. Potok, C. M. Marcus, and V. Umansky, *Science* **299**, 5607 (2003).

¹⁷ J. R. Hauptmann, J. Paaske, and P. E. Lindelof, *Science* **4**, 373 (2008).

¹⁸ M. Yamamoto, T. Ohtsuki, and B. Kramer, *Phys. Rev. B* **72**, 115321 (2005).

¹⁹ A. W. Cummings, R. Akis, and D. K. Ferry, *Appl. Phys. Lett.* **89**, 172115 (2006).

²⁰ A. W. Cummings, R. Akis, D. K. Ferry, J. Jacob, T. Matsuyama, U. Merkt, and G. Meier, *J. Appl. Phys.* **104**, 066106 (2008).

²¹ P. Földi, O. Kálmán, M. G. Benedict, and F. M. Peeters, *Phys. Rev. B* **73**, 155325 (2006).

²² A. T. Ngo, P. Debray, and S. E. Ulloa, *Phys. Rev. B* **81**, 115328 (2010).

²³ M. Kohda, S. Nakamura, Y. Nishihara, K. Kobayashi, T. Ono, J. O. Ohe, Y. Tokura, T. Mineno, and J. Nitta, *Nature Communications* **3**, 1082 (2012).

²⁴ M. I. D'yakonov and V. I. Perel, *Sov. Phys. Solid State* **13**, 3023 (1971).

²⁵ D. Chang, G. L. Khym, K. Kang, Y. Chung, H. J. Lee, M. Seo, M. Heiblum, D. Mahalu, and V. Umansky, *Nature Physics* **4**, 205 (2008).

²⁶ C. W. Groth, M. Wimmer, A. R. Akhmerov, and X. Waintal, arXiv:1309.2926.

²⁷ S. Datta, *Electronic transport in mesoscopic systems* (Cambridge University Press, 1995).

²⁸ T. Ando, Phys. Rev. B **44**, 8017 (1991).

²⁹ G. Engels, J. Lange, T. Shäpers, and H. Lüth, Phys. Rev. B **55**, 1958(R) (1997).